山口大学教育学部研究論叢　第 75 巻　213 頁～ 223 頁　2026 年 1 月

Visualization of the Particulate and Kinetic Nature of Matter by Utilization of Physical Models, Part III: van der Waals Gas, and Dimerization and Recombination Reactions

MURAKAMI Kiyofumi（村上清文）, KOMATSU Yusuke（小松裕典）,
FUJIMURA Taihei（藤村泰平）, WAIZUMI Kenji（和泉研二）

（Received September 26, 2025）

ABSTRACT

This paper describes applications of a molecular-movement presentation apparatus, which was constructed to visualize particulate and kinetic nature of matter, to chemically interacting systems such as a van der Waals gas and dimerization and recombination reactions. Regarding the van der Waals gas, *P-V* curves were measured for two model systems with different interaction strengths. A peak behavior characteristic of the van der Waals gas equation of state was observed within a suitable range of interaction strength and temperature. This peak behavior in *P-V* curve observed in the present model system is interesting from the viewpoint of the relationship between system size and observable state, that is a metastable or an unstable state in macroscopic systems may exist stably in a microscopic small number of particles system. Regarding the dimerization and recombination reactions, it became possible to determine temperature dependence of the equilibrium constant by measuring the concentrations of all species present in the system over a wide temperature range, and the internal energy change of reaction has been evaluated. Furthermore, it became possible to draw an activation energy profile of dimerization from the time-dependent data of the reaction. These results suggest that learning with these model systems will lead to a deeper understanding of van der Waals gas and dimerization and recombination reactions and to improving students' various misconceptions about chemical reactions.

1. INTRODUCTION

Understanding the particulate and kinetic nature of matter is essential to promote students' conceptual understanding of chemical phenomena. However, many assessment studies have shown that this is difficult for students. As a result, many students retain various misconceptions about the fundamental properties of matter. For example, matter is a continuous medium with no empty space between particles (Novick & Nussbaum, 1978, Novick & Nussbaum, 1981, Griffiths & Preston, 1992), gas is weightless (Furio Mas et al., 1987, Stavy, 1988), molecules expand when heated (Novick & Nussbaum, 1981, Griffiths & Preston, 1992, Lin & Lawrenz, 2000), etc. Such misconceptions are stubborn and survive through many stages of instruction, and even after a course of instruction has been completed (Novick & Nussbaum, 1981, Stavy, 1988), e.g. even chemistry teachers find that it is not easy to solve conceptual problems (Lin & Lawrenz, 2000).

Furthermore, it has become clear that many students have some difficulties with chemical equilibrium, such as difficulty understanding the dynamic nature (Gussarsky & Gorodetsky, 1986, Ozmen, 2008) and reversible feature of chemical equilibrium (Maskill & Cachapuz, 1989, Berquist & Heikkinen, 1990, Ozmen, 2008), confusion between reaction rate and extent of

Department of Science, Faculty of Education, Yamaguchi University, Yoshida 1677-1, Yamaguchi 753, Japan

reaction (Hackling & Garnett, 1985, Banerjee, 1991), difficulty understanding the constancy of the equilibrium constant (Wheeler & Kass, 1978, Voska & Heikkinen, 2000), and incorrect application of Le Chatelier's principle (Tyson et al., 1999, Solomonidou & Stavridou, 2001).

In recent years, Murakami et al. (2021a, 2021b) have been trying to develop educational materials that promote conceptual understanding of chemical phenomena by visualizing particulate and kinetic behavior using physical models of atoms and molecules. They proposed a molecular motion presentation apparatus that can directly measure macroscopic physical quantities such as pressure and volume, while expressing microscopic molecular motion using superballs as physical model molecules. It was clarified that by using this apparatus, it became possible to visualize the microscopic thermal motion of gas molecules, and to show the relationship between macroscopic quantities and microscopic molecular motions, and the relationship between macroscopic quantities expressed by gas law ($PV = nRT$) (Murakami et al., 2021a).

Furthermore, as a result of applying the apparatus to chemically interacting systems of a bimolecular binding reaction, it became possible to present the kinetic and reversible nature of chemical equilibrium, the internal energy changes of reaction, the constancy of equilibrium constants, and the approach from a non-equilibrium state to the equilibrium one (Murakami et al., 2021b). These results suggest that the present visualization approach using physical models is helpful in improving above mentioned students' misconceptions about chemical equilibrium, and further raise the expectation that it may also be applied to more complicated chemical reaction systems.

In this study, physical models of van der Waals gas imitating water molecule, dimerization reaction and recombination reaction were constructed. In addition to observability of the microscopic and kinetic nature of these systems, macroscopic thermodynamic quantities such as the P-V curve and equilibrium constant were examined. Based on the results, the possibility of applying these model systems to chemistry education was discussed.

2. EXPERIMENTAL

2.1 van der Waals gas models

2.1.1 Weak interaction model.

A superball with a diameter of 21 mm and a weight of 4.6 g was used for a weakly interacting van der Waals molecular model. In this model, a cylindrical ferrite magnet with a thickness of 2 mm and a diameter of 5 mm were embedded in each of the six vertices of the regular octahedron inscribed in the superball so that the three S poles and three N poles were directed outward. Total weight of the model molecule was 6.4 g. Figure 1 shows the conceptual diagram and the photograph of the weak interaction model.

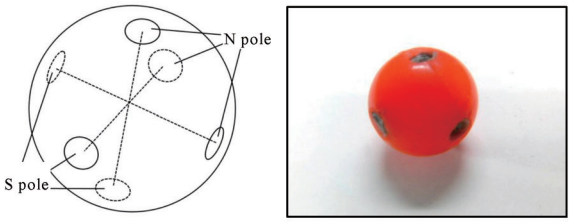

Figure 1. Conceptual diagram and an actual photograph of the weak-interaction model.

2.1.2 Strong interaction model.

The same superball was used for a strongly interacting van der Waals molecular model. A cylindrical neodymium magnet with a length of 6 mm and a diameter of 3 mm was used to realize the interaction. Holes with a depth of 5 mm were made at the four vertices of the regular tetrahedron inscribed in the superball, and magnets were embedded so that two N poles and two S poles protruded 1 mm from the surface. The weight of the model molecule became 5.6 g. Considering the valence shell electron pair repulsion rule, this model can also be considered as a model of water molecule. Figure 2 shows the conceptual diagram and the photograph of the model.

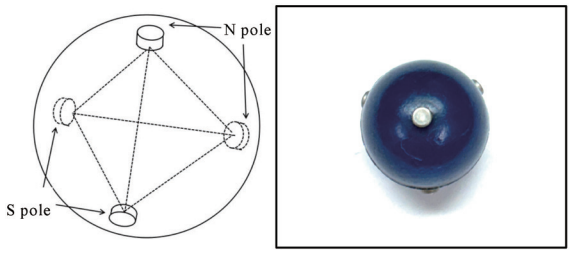

Figure 2. Conceptual diagram and an actual photograph of the strong-interaction model.

2.1.3 Non-interaction model.

In order to compare the behavior of interacting and non-interacting model molecule systems, a non-interaction

model (perfect gas model) was also created, in which a copper column with 5mm diameter was embedded instead of magnets and the weight of the model made equal to that of the interaction models. Figure 3 shows the conceptual diagram and the photograph of the non-interaction model.

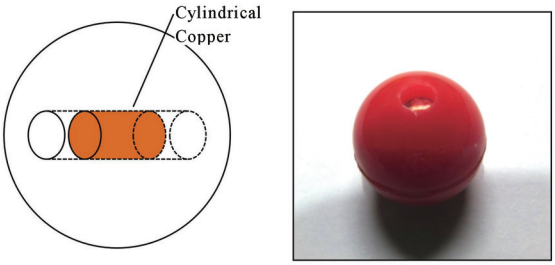

Figure 3. Conceptual diagram and an actual photograph of the non-interaction model.

2.2 Dimerization and recombination model

The monomer model A was created by drilling a hole 5 mm diameter and 5 mm depth in the surface of the superball (diameter=20mm, weight=3.9g) and embedding three magnets (cylindrical neodymium magnet: 6mm length and 2.5mm diameter) in it, with two north poles and one south pole protruding from the surface. This allowed us to represent the dimer A_2 by binding two of the three embedded magnets to the other's two magnets. Figure 4 shows the conceptual diagram of the monomer and actual photograph of the dimer.

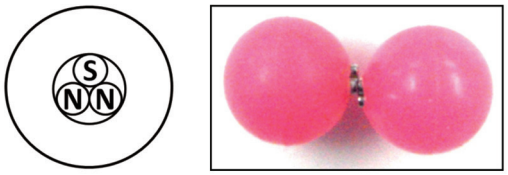

Figure 4. Conceptual diagram of monomer model and photograph of the dimer.

Similar to the A molecule model, the B molecule model used three magnets and was embedded so that one N pole and two S poles were exposed. This made it possible to express the dimer B_2 in the same way as the dimer A_2. Furthermore, it is possible to represent a recombination reaction in which A_2 and B_2 molecules dissociate and A and B bind to each other to form AB, in which all three magnets of A can bind to those of B, so that the bonding force of AB is stronger than that of A_2 and B_2.

2.3 Measurements

An appropriate number of model molecules were placed in the container of the molecular-movement presentation apparatus (Murakami et al., 2021a). Then the model system was thermally excited by reciprocating the base plane with triangular prisms. Temperature was evaluated from the relation between mean square kinetic energy of super balls and temperature

$$\frac{1}{2}m\overline{v^2}=\frac{3}{2}k_BT \tag{1}$$

and the relation between the mean square speed and the square of the most probable speed, which was assumed to be the same with the maximum speed of the reciprocating base plane (Murakami et al., 2021a).

$$\overline{v^2}=(3/2)\,v_m{}^2 \tag{2}$$

Measurements for the van der Waals gas model were performed with 20 model molecules. Under a constant temperature (keeping the frequency of the reciprocating base plane to be a constant value), the pressure was measured each time while changing the volume of the system. The measurements were performed at four temperatures by changing the reciprocating-speed adjustment scale of the device. After a series of measurements, P-V curves were plotted for each temperature.

Concerning the measurements for the dimerization reaction model, 14 A_2 model molecules were placed in the molecular-movement presentation apparatus, and thermal motion was excited under a constant volume. After equilibration, many snapshots (typically fifty shots) of the reaction system were taken using a high-speed digital camera EX-FH20 Casio Co., Ltd. For each picture, the numbers of existing species were counted. Then, the average number and its standard deviation for each species were calculated over all snapshot pictures. The concentrations of the species were calculated by dividing the average numbers by the volume of the reaction container of the apparatus. In the present study, all the experiments were performed at a constant volume of 11.925 dm^3. For the measurements of recombination reaction model, 7 A_2 model molecules and 7 B_2 model molecules were placed in the apparatus. The measurement procedure was the same as that for the dimerization reaction model.

3. RESULTS and DISCUSSION

3.1 van der Waals gas model

Van der Waals equation of state is the equation that takes into account the attractive interaction between molecules and the size of molecule.

$$\left(P+\frac{n^2a}{V^2}\right)(V-nb)=nRT \tag{3}$$

where P and V are the pressure and volume of gas respectively, n is the number of moles of gas molecules, R is gas constant, T is absolute temperature, and a is the parameter representing intermolecular interaction and b is the excluded volume occupied by 1 mole of molecule.

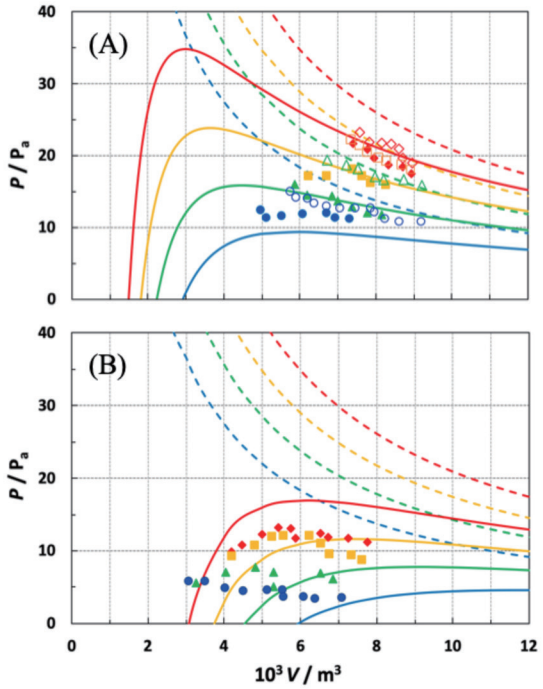

Figure 5. P vs V plots for the weak interaction system (A) and the strong interaction system (B). Open symbols and broken curves show the data and the theoretical curves for the non-interaction model, respectively. Filled symbols and solid curves show the data and the theoretical curves for the weak and strong interaction systems. The colors mean temperature; blue: 3.86×10^{20} K, green: 5.02×10^{20} K, orange: 6.12×10^{20} K, red: 7.35×10^{20} K.

When there is no intermolecular interaction and no molecular size, i.e., a=0 $P_a m^6 mol^{-2}$ and b=0 m^3, this equation becomes the equation of state of perfect gas ($PV=nRT$). Expressing the volume dependence of pressure by using the number of particles N in the system is as follows.

$$P=\frac{Nk_BT}{V-Nb/L_0}-\frac{a}{V^2(L_0/N)^2} \tag{4}$$

Where L_0 is Avogadro's constant. Since the value of b can be evaluated as 2.92×10^{18} m^3 from the product of the volume of one model sphere and L_0, a becomes the only one parameter for a given N.

Figure 5 shows the P vs V plots for the weak and the strong interaction systems. The value of a was evaluated as the value at which the theoretical curves at the four temperatures fit the experimental data. The values of a evaluated for the weak and the strong interaction systems are 3.0×10^{41} $P_a m^6 mol^{-2}$ and 6.0×10^{41} $P_a m^6 mol^{-2}$, respectively. Despite the fact that the number of parameters is only one, the theoretical curves seem to reproduce the experimental data well.

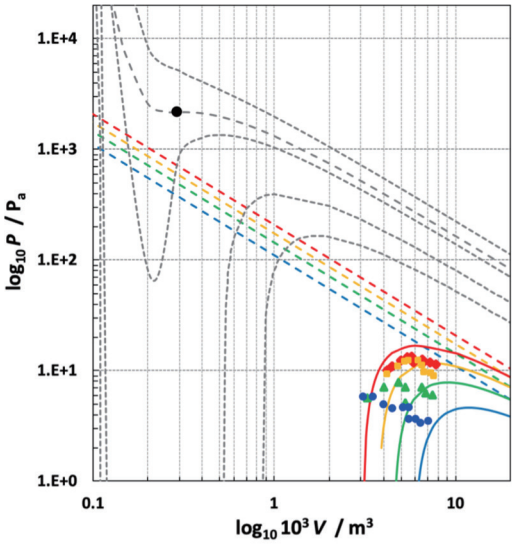

Figure 6. Wide area plot of P vs V including critical point for the strong interaction system. The filled symbols and solid lines are the data and van der Waals theoretical curves for the strong interaction system. The broken lines show the graphs for the perfect gas with a=0 $P_a m^6 mol^{-2}$ and b=0 m^3. The black dot indicates the position of the critical point.

Furthermore, by setting the first and second derivatives of P with respect to V to be zero, we can calculate the position of the critical point as,

$$V_c=3\cdot\frac{N}{L_0}\cdot b \tag{5}$$

$$T_c=\frac{2}{3k_B}\cdot\frac{8a}{27b}\cdot\frac{N}{L_0} \tag{6}$$

$$P_c = \frac{a}{27b^2} \quad (7)$$

The critical point of the strong interaction system was estimated as, P_c=2.17×10^3 Pa, V_c=2.91×10^{-4} m^3, T_c=1.22×10^{23} K. Figure 6 shows a logarithmic graph plotting the relationship between volume and pressure at multiple temperatures, including the critical point for the strong interaction model. For comparison, the graph for a perfect gas with a=0 Pa m^{6}mol^{-2} and b=0 m^3 are also plotted.

3.1.1 *Educational meaning of the results for the van der Waals gas model.*

The following points can be confirmed from these figures. First, the pressure in the interacting systems is smaller than that in the non-interacting system. Furthermore, the pressure in the strong interaction system is much smaller than that in the weak interaction system. Second, the pressures in the non-interacting and weakly interacting systems are decreasing functions of volume in the observed region, whereas the curves of the volume dependence of pressure in the strong interaction system have a maximum point for some temperature values. The position of this maximum point roughly matches with that of the theoretical curves. Looking more closely, such peak behavior was observed at relatively high temperatures, and when the temperature is lowered, the peak disappears, and the pressure changes little or increases slightly even if the volume decreases.

The van der Waals equation of state is often taken up as an advanced topic in upper secondary school chemistry (Takeuchi et al., 2021), a subject in general chemistry at the first year of university (Brown et al., 2014) and that in more specialized field of physical chemistry (Atkins et al., 2024), as it expresses the behavior of real gases from theoretical and phenomenological viewpoints. There, the effects of excluded volume and of pressure reduction due to the presence of interaction between molecules are described. In particular, the P-V curve is explained as follows (Takeuchi et al., 2021). Boyle's law is obeyed until condensation due to interaction begins, but when condensation begins due to volume reduction, pressure becomes constant at the saturated vapor pressure and condensation progresses. When all the gas becomes liquid, pressure rises sharply. This P-V curve behavior associated with condensation originates from the macroscopic nature of the system. Therefore, the peak behavior predicted by the van der Waals equation of state would never be observed for real gases, since the region where the compressibility is negative $\left(-\frac{1}{V}\left(\frac{dV}{dP}\right)_T < 0\right)$ is a thermodynamically unstable state. In fact, such peak behavior has not been observed in real gas systems (Mayrhuber, 2021).

With this in mind, the peak behavior in the P-V curves observed in the present model system is interesting from the viewpoint of the relationship between system size and observable quantities. That is, in microscopic systems consisting of a small number of interacting particles, it may be possible to observe the characteristic behavior of the van der Waals equation of state, where as the volume decreases pressure increases, passes through a peak, and then decreases. This means that a metastable or unstable state in a macroscopic system might exist stably in a microscopic small number of particles system. We don't know any real examples of van der Waals gas (gases that follow the van der Waals equation of state), but the present model-molecular system might be said to be a real example of van der Waals gas, although it just be a model system. By combining the present device with model molecular systems that interact with each other and teaching from the above perspectives, it is believed that it will be possible to contribute to deeper understanding of the P-V curve behavior of interacting particle systems.

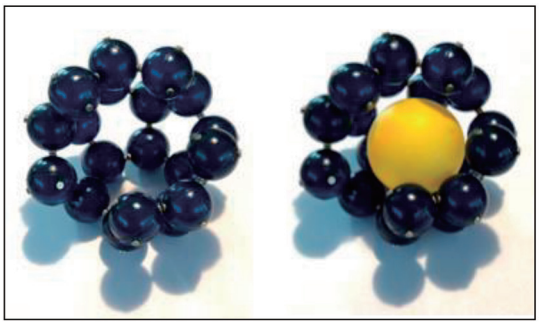

Figure 7. A cage-like structure (substructure of tetradecahedral 5^{12}, 6^2 cage structure (Arata, 1998)) formed under a low temperature condition. On the left is the formed cage structure, and on the right is a structure with a table tennis ball inside to make the space easier to see.

Furthermore, it is interesting that we were also able to observe the formation of a water-specific cage-like

structure under low-temperature conditions for a system of 30 strong interaction model molecules (Fig. 7). Being able to actually see such structures in students' hands is likely to be of great value in chemical education.

3.2 Dimerization and recombination model

The dimer formation reaction of A molecules can be expressed by the next equation.

$$2A \overset{K_A}{\longleftrightarrow} A_2 \tag{8}$$

When B molecules coexist, the following two reactions must be considered.

$$2B \overset{K_B}{\longleftrightarrow} B_2 \tag{9}$$

$$A+B \overset{K_{AB}}{\longleftrightarrow} AB \tag{10}$$

The equilibrium constants for these reactions can be expressed by the following equations.

$$K_A = \frac{[A_2]}{[A]^2} \tag{11}$$

$$K_B = \frac{[B_2]}{[B]^2} \tag{12}$$

$$K_{AB} = \frac{[AB]}{[A][B]} \tag{13}$$

Where the concentrations were defined by number concentration instead of ordinary mole concentration, as

$$[A] = \frac{Number\ of\ A}{Volume\ of\ model\ gas} \tag{14}$$

Figure 8 shows the temperature change in the number of each species when total number of 14 A_2 model molecules exist in the system. We can see from this figure that as the temperature rises, the dissociation of dimers proceeds and the number of monomers increases.

Figures 9 shows the snapshot picture and the temperature dependence of the number of existing species in the case of coexisting B. From this figure, it can be seen that AB predominates at low temperatures and the number of monomers becomes dominant as the temperature increases. The numbers of A_2 and B_2 are low at all temperatures.

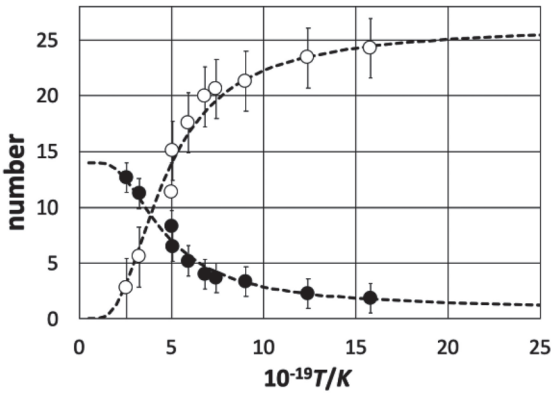

Figure 8. Temperature dependence of the number of existing species, when total number of 14 A_2 model molecules were set in the system. Open circle shows the number of A and the filled circle shows that of A_2. The error bar shows standard deviation of each data.

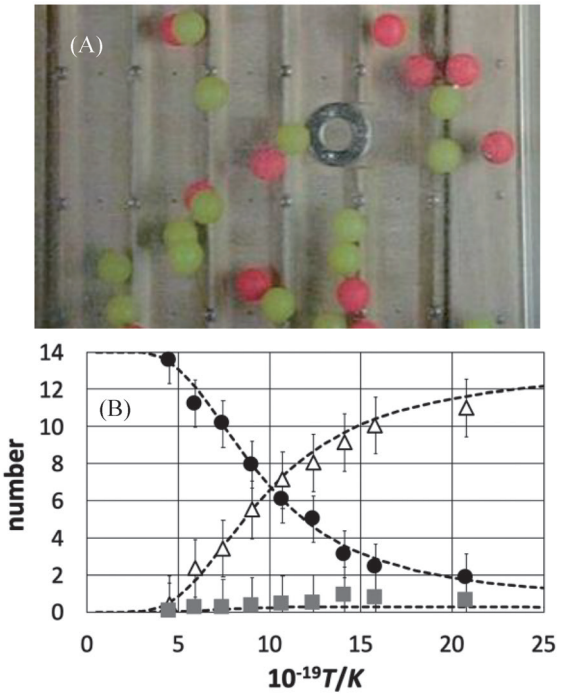

Figure 9. (A): A snapshot picture observed when A and B coexist. The numbers of A_2 (yellow ball) and B_2 (pink ball) were set equally to 7. (B): Temperature dependence of the number of existing species. The symbols show A (triangle), A_2 (gray square) and AB (black circle). The error bar shows standard deviation of each data.

From the data on the temperature dependence of the equilibrium constant determined using equations from (11) to (13), the internal energy change of the reaction (ΔU) can be evaluated using the Van't Hoff equation (Berry et al., 1980),

$$\ln K = -\frac{\Delta U}{R} \cdot \frac{1}{T} + C \tag{15}$$

Figure 10 shows van't Hoff plots for the dimerization and the complex formation reactions. From this figure, we can see that the data are on a good linear relationship. From the slopes of these lines, the internal energy changes for the dimerization and the complex formation have been evaluated as -1.63×10^{21} Jmol^{-1} and -3.95×10^{21} Jmol^{-1}, respectively. The negative sign of these values indicates that these reactions are exothermic.

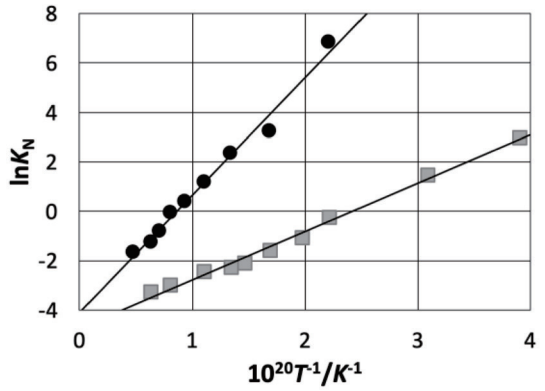

Figure 10. van't Hoff plots of the dimerization (gray square) and the complex formation (black circle) reactions. The solid lines are the best fit ones to those data.

The activation energies for the dimer formation can be evaluated from time-dependent reaction curve. Figure 11 shows the time course of the number of A_2.

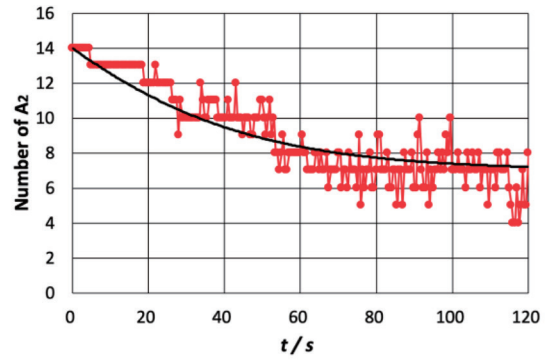

Figure 11. Time course of the number of A_2 after the temperature-jump measurement. The solid line is the best fit theoretical curve to the data.

Fourteen A_2 molecular models were put into the molecular motion presentation device, and the initial temperature was set to the temperature where all the existing species are in A_2 form, and then the temperature was suddenly raised to the equilibrium temperature (T=5.07×10^{19} K) at which the number of A_2 is 7.

After this rapid temperature rise, pictures of the reaction system were taken every 0.5 seconds, and the time course of the number of species present was measured. This is called temperature-jump measurement (Hiromi, 1979). This time course of A_2 can be expressed by the next equation (see Appendix 1).

$$[A_2](t)=\left\{\overline{[A_2]}-\frac{\Delta[A_2]^0 e^{-\frac{t}{\tau}}}{1+4K_A k_{-1}\Delta[A_2]^0\tau(1-e^{-\frac{t}{\tau}})}\right\}\times V \qquad (16)$$

, where k_{-1} is the backward rate constant in Eq. 8, the dimerization constant K_A was evaluated as 0.341×10^{21} $N^{-1}dm^3$, and

$$\frac{1}{\tau}=4K_A k_{-1}\overline{[A]}+k_{-1} \qquad (17)$$

$\Delta[A_2]^0$ means the difference between initial concentration $[A_2]^0$ and equilibrium concentration $\overline{[A_2]}$

$$\Delta[A_2]^0=\overline{[A_2]}-[A_2]^0 \qquad (18)$$

Equation 16 was fitted to the data with k_{-1} as a parameter. As a result, the value of k_{-1} was evaluated as k_{-1}=0.011 s^{-1}. Using this value and that of K_A, value of k_1 was calculated as k_1=0.00375 N^{-1}dm^3s^{-1}. From these values, free energy of dimerization and activation energies have been estimated as $\Delta G=-RT\ln K_A$ =0.453×10^{21} Jmol^{-1}, $\Delta G_1^{\ddagger}=-RT\ln k_1$=2.26×10^{21} Jmol^{-1} and $\Delta G_{-1}^{\ddagger}=-RT\ln k_{-1}$=1.90×10^{21} Jmol^{-1}. The free energy profile of the system can be depicted as in Figure 12.

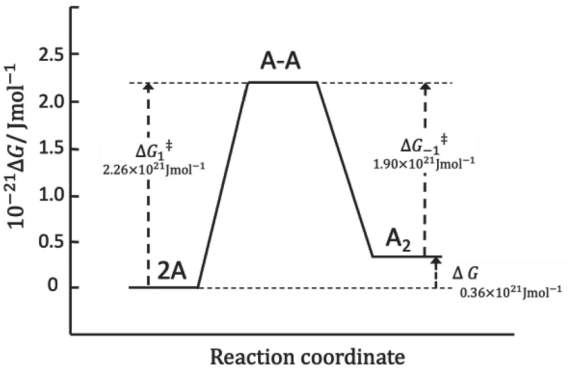

Figure 12. Free energy profile of the dimerization reaction of the present model system. T=5.07×10^{19} K

3.2.1 Implications of the dimerization and recombination model in chemical education.

In the field of chemical reactions, students have the following misconceptions (Garnett et al., 1995, Lin & Lawrenz, 2000, Nakhleh, 1992). 1) Dynamic aspects of

chemical equilibrium, i.e., at equilibrium, no chemical reaction is occurring (Mc.1). 2) At equilibrium, the amounts of reactants and products are equal (Mc.2). 3) The reaction proceeds until the reactants are consumed (Mc.3). 4) The constancy of the equilibrium constant is difficult to understand, i.e., when the amount of substance changes, the equilibrium constant changes (Mc.4). 5) Students write incorrect chemical equations, i.e., when expressing $N_2 + 3H_2 \rightarrow 2NH_3$, $3H_2$ is expressed as H_6 and $2NH_3$ is expressed as N_2H_6 (Mc.5).

Murakami et al. (1921b) prepared a physical model of bimolecular binding reaction, representing the next formula.

$$A+B \leftrightarrow C \tag{19}$$

They proposed the following situations in which this model could be applied to educational practice in the field of chemical reactions. First, by showing the total amount of atoms remains the same before and after the reaction, we can use the model to promote particulate and conceptual understandings concerning chemical changes and constancy of mass. Second, it is possible to demonstrate Le Chatelier's principle regarding temperature changes and to calculate quantitatively the equilibrium constant, thereby showing the dynamic aspects of the equilibrium state. By using this model as a teaching material, it was thought that the model will contribute to the elimination of the above misconceptions from Mc.1 to Mc.4.

These misconceptions can also be resolved by using the present dimer formation reaction model, where interconversion between monomer and dimer states can be seen visually and microscopically in a thermal equilibrium state. Model molecules frequently collide to each other resulting some times in formation of dimer A_2 from two A molecules or in decomposition of A_2 to two A molecules. It was also observed that A_2 acquires rotational motion around its center of gravity. It can be seen that the dimer formation and its decomposition into monomers do not occur with every collision with other molecules, but when the mutual approaching speed and orientation are within an appropriate range. Demonstrating these behaviors under chemical equilibrium will contribute to the visual and conceptual understandings of the kinetic nature of chemical equilibrium.

In textbooks of upper secondary school chemistry (Takeuchi et al., 2021), general chemistry at the first year of university (Brown et al., 2014) and physical chemistry (Atkins et al., 2024), the next reaction is treated as a representative example of Eq. 8.

$$2NO_2 \leftrightarrow N_2O_4 \tag{20}$$

This reaction is often treated as an example to explain Le Chatelier's principle in the field of chemical equilibrium. This reaction is exothermic. This is an effective reaction in chemical education because it can visually show the change in color of a gas caused by an increase or decrease in reddish-brown NO_2 or colorless N_2O_4 due to an equilibrium shift by temperature change. This reaction is suitable for qualitatively demonstrating the shift in chemical equilibrium due to temperature and pressure, but it is difficult to quantitatively show the change in equilibrium constant.

In contrast to this, our dimer formation model makes it possible to quantitatively evaluate the temperature dependence of the equilibrium constant, as shown in the previous section. Of course, the pressure dependence is also possible. Furthermore, measuring time evolution of reactive species in real systems requires special apparatus and measurement techniques, such as the stopped-flow and relaxation methods (Hiromi, 1979). In contrast, by using the present apparatus and the physical model, anyone can track the time course of a reaction by taking photographs and counting the number of particles. Furthermore, by following the series of procedures described in the previous section, anyone can learn how to experimentally determine rate constants and activation energies.

In further, by using the dimer-molecules-recombination reaction model created in this study, it will become possible to demonstrate the reaction expressed by the equation.

$$A_2+B_2 \leftrightarrow 2AB \tag{21}$$

This reaction model will make it possible to resolve Mc.5. A teacher confirms with his students that the A_2 and B_2 molecular models are in the form of dimer, and then puts the same amounts of models into the device and shows the reaction of Eq. 21. Once almost all of the dimer molecular models have been transformed into the

complexes by recombination, they can confirm that the product formed is AB instead of A_2B_2 and that the number of complexes is twice the number of each dimer model initially added. This allows them for an understanding of the meaning of coefficients of chemical reaction equations, and that molecules do not bond continuously as shown in Mc.5, but the number of bonds is fixed to a definite number. This is thought to lead further to the understanding of valence, which means that each atom has a fixed number of valence electrons that can be used for covalent bonds. As this type of reaction, the following reactions are often described in text books (Takeuchi et al., 2021, Brown et al., 2014, Atkins et al., 2024);

$$H_2+I_2 \leftrightarrow 2HI \quad (22)$$

$$H_2+Cl_2 \leftrightarrow 2HCl \quad (23)$$

$$N_2+O_2 \leftrightarrow 2NO \quad (24)$$

Although the detailed mechanisms differ to each other, improvements to the present model will enable us to describe these reactions as well.

Additionally, it has been reported that students are often unable to quantitatively understand reactions when one of the reactants is in excess or insufficient (Garnett et al., 1995, Lin & Lawrenz, 2000, Nakhleh, 1992). In order to facilitate quantitative understanding of reaction, we can also use this model when unequal numbers of A_2 and B_2 molecular models are placed in the device. At that time, students can easily learn the concept of a limiting reagent by focusing on the fact that the amount of produced product is determined by the amount of a smaller amount of reactant.

From the above consideration, we can see that the combination of this device and some model molecular systems contributes to the student's conceptual understanding of chemical equilibrium and kinetics, because it allows the visualization of structural changes of molecules as a real model and the quantitative evaluation of physical quantities by counting the number of particles.

4. SUMMARY

By using the molecular-movement presentation apparatus together with the physical models of van der Waals gas and dimerization and recombination reactions, it became possible to visualize the particulate and kinetic nature of these interacting systems.

Concerning the van der Waals gas model mimicking water molecules, pressure reduction due to the presence of interaction between molecules was presented by the model system and in further the characteristic peak behavior of the van der Waals equation of state was observed in an appropriate temperature range for the present microscopic small number of particles system, that cannot be observed in macroscopic systems. Furthermore, a water-specific cage-like structure was found to be formed under low-temperature conditions. Concerning the dimerization reaction model, we were able to determine the binding constants by counting the species present in snapshots taken with a high-speed digital camera at equilibrium at a certain temperature. Furthermore, by collecting data at different temperatures, we were able to calculate the internal energy change of dimerization using van't Hoff plots. Furthermore, by analyzing the time dependence of the dimer formation reaction, we demonstrated that it is possible to draw a free energy profile including the activated state. It was also found that the recombination reaction of dimers could be described by this model.

Based on these results, it was expected that the combination of this device and some reaction models in teaching will help students improve various misconceptions about chemical reactions, and will also enable them to learn kinetic analysis, such as visualizing the dynamic and kinetic nature of chemical equilibrium, the temperature dependence of the equilibrium constant and the approach from non-equilibrium states to the equilibrium state, which would normally require special equipment and techniques.

REFERENCES

Arata Y (1998) Book of Water, Kyoritsu Publishing (in Japanese).

Atkins P et al. (2024) Atkins' Physical Chemistry (12th edition), Oxford University Press.

Banerjee AC (1991) Misconceptions of students and teachers in chemical equilibrium. *Int J Sci Educ* **13**, 487-494.

Berquist W, Heikkinen H (1990) Student ideas regarding chemical equilibrium. *J Chem Educ* **67**, 1000-1003.

Berry RS, Rice SA, Ross J (1980) Physical Chemistry

(John Wiley & Sons, 1980), p762.

Brown TL et al. (2014) Chemistry: The Central Science (13th Edition), Pearson

Furio Mas CJ, Perez JH, Harris HH (1987) Parallels between adolescents' conception of gases and the history of chemistry. *J Chem Educ* **64**, 616-618.

Garnett PJ, Garnett PJ, Hackling MW (1995) Students' alternative conceptions in chemistry: A review of research and implications for teaching and learning. *Studies in Sci Educ* **25**, 69-95.

Griffiths AK, Preston KR (1992) Grade-12 students' misconceptions relating to fundamental characteristics of atoms and molecules. *J Res Sci Teach* **29**, 611-628.

Gussarsky M, Gorodetsky E (1986) Misconceptualization of the chemical equilibrium concept as revealed by different evaluation methods. *Eur J Sci Educ* **8**, 427-441.

Hackling MW, Garnett PJ (1985) Misconceptions of chemical equilibrium. *Eur J Sci Educ* **7**, 205-214.

Hiromi K (1979) Kinetics of Fast Enzyme Reactions: Theory and Practice, John Wiley & Sons, New York, ISBN 0-470-26866-2

Lin H-S, Cheng H-J, Lawrenz F (2000) The assessment of students and teachers' understanding of gas laws. *J Chem Educ* **77**, 235-238.

Maskill R, Cachapuz AF (1989) Learning about the chemistry topic of equilibrium: The use of word association tests to detect developing conceptualizations. *Int J Sci Educ* **11**, 57- 69.

Mayrhuber F (2021) Analysis of p, T, ρ-data for all fluid states via comparison with a transcribed Van der Waals equation. *Chemical Thermodynamics and Thermal Analysis* 1-2 (2021) 100003

Murakami K, Sugimoto T, Waizumi K (2021a) Visualization of the particulate and kinetic nature of matter by utilization of physical models, Part I: Gas laws. *Aust J Ed Chem* **78**, 1-8.

Murakami, K., Komatsu, Y., Waizumi, K. (2021b) Visualization of the particulate and kinetic nature of matter by utilization of physical models, Part II: Chemical equilibrium. *Aust J Ed Chem* **78**, 9-15.

Nakhleh MB (1992) Why some students don't learn chemistry. *J Chem Educ* **69**, 191-196.

Novick S, Nussbaum J (1978) Junior high school pupils' understanding of the particulate nature of matter: An interview study. *Sci Educ* **62**, 273-281.

Novick S, Nussbaum J (1981) Pupils' understanding of the particulate nature of matter: A cross-age study. *Sci Educ* **65**, 187- 196.

Ozmen H (2008) Determination of students' alternative conceptions about chemical equilibrium: A review of research and the case of Turkey. *Chem. Educ Res Pract* **9**, 225-233.

Solomonidou C, Stavridou H (2001) Design and development of a computer learning environment on the basis of students' initial conceptions and learning difficulties about chemical equilibrium. *Educ Inf Tech* **6**, 5-27.

Stavy R (1988) Children's conception of gas. *Int J Sci Educ* **10**, 553-560.

Takeuchi Y et al. (2021) Revised Chemistry (Textbooks of chemistry approved by the Ministry of Education), Tokyo Shoseki (in Japanese).

Tyson L, Treagust DF, Bucat RB (1999) The complexity of teaching and learning chemical equilibrium. *J Chem Educ* **76**, 554-558.

Voska KW, Heikkinen HW (2000) Identification and analysis of student conceptions used to solve chemical equilibrium problems. *J Res Sci Teach* **37**, 160-176.

Wheeler AE, Kass H (1978) Student misconceptions in chemical equilibrium. *Sci Educ* **62**, 223-232.

Appendix: Derivation of the time dependence of $[A_2](t)$ in the dimer formation reaction

The reaction curve from the initial state of the reaction to the equilibrium state can be obtained as follows.

$$2A \underset{k_{-1}}{\overset{k_1}{\rightleftarrows}} A_2 \tag{A-1}$$

Here, the equilibrium constant K_1 is given by the next equation and is assumed to be known from the results of equilibrium measurements.

$$K_1 = \frac{k_1}{k_{-1}} = \frac{\overline{C_{A_2}}}{\overline{C_A}^2} \tag{A-2}$$

Here, the superscript $-$ indicates equilibrium. The deviation of the concentrations of A and A_2 from their equilibrium concentrations is defined by the following equations:

$$\Delta C_A = \overline{C_A} - C_A \tag{A-3}$$
$$\Delta C_{A_2} = \overline{C_{A_2}} - C_{A_2} \tag{A-4}$$

From the stoichiometric relationship in Eq. A-1, the next relationship holds between ΔC_A and ΔC_{A_2},

$$\Delta C_A = -2\Delta C_{A_2} = -2\Delta C \tag{A-5}$$

Here, ΔC was defined as

$$\Delta C \equiv \Delta C_{A_2} \tag{A-6}$$

Using these, C_A and C_{A_2} can be expressed as follows:

$$C_A = \overline{C_A} - \Delta C_A = \overline{C_A} + 2\Delta C \tag{A-7}$$
$$C_{A_2} = \overline{C_{A_2}} - \Delta C_{A_2} = \overline{C_{A_2}} - \Delta C \tag{A-8}$$

The rate equation for C_{A_2} becomes

$$\frac{dC_{A_2}}{dt} = k_1 C_A^{\,2} - k_{-1} C_{A_2} \tag{A-9}$$

Substituting Eqs. A-7 and A-8 into Eq. A-9, we get

$$-\frac{d\Delta C}{dt} = (4k_1\overline{C_A} + k_{-1})\Delta C + 4k_1\Delta C^2 \tag{A-10}$$

The solution to this differential equation is given by the following equation (Hiromi, 1979):

$$\Delta C(t) = \frac{\Delta C^0 e^{-\frac{t}{\tau}}}{1 + 4k_1\Delta C^0\tau(1 - e^{-\frac{t}{\tau}})} \tag{A-11}$$

Here,

$$\frac{1}{\tau} = 4k_1\overline{C_A} + k_{-1} \tag{A-12}$$

$$\Delta C^0 = \overline{C_{A_2}} - C^0_{A_2} \tag{A-13}$$

where, $C^0_{A_2}$ is the concentration of A_2 at t=0. Using this solution, the change in A_2 concentration over time is given by

$$C_{A_2}(t) = \overline{C_{A_2}} - \Delta C(t) \tag{A-14}$$

and the change in the number of A_2 over time is given by

$$A_{2N}(t) = C_{A_2}(t) \times V \tag{A-15}$$

Rewriting equations (A-11) and (A-12) using K_1 gives

$$\Delta C(t) = \frac{\Delta C^0 e^{-\frac{t}{\tau}}}{1 + 4K_1k_{-1}\Delta C^0\tau(1 - e^{-\frac{t}{\tau}})} \tag{A-16}$$

That is, the changes in the concentration and number of A_2 over time can be expressed using equations A-16, A-12, A-14, and A-15.